Impact of dimethylsulfide chemistry on air quality over the Northern Hemisphere

Junri Zhao[1], Golam Sarwar[2], Brett Gantt[3], Kristen Foley[2], Barron H. Henderson[3], Havala O. T. Pye[2], Kathleen Fahey[2], Daiwen Kang[2], Rohit Mathur[2], Yan Zhang[1], Qinyi Li[4], Alfonso Saiz-Lopez[4]

[1] Shanghai Key Laboratory of Atmospheric Particle Pollution and Prevention (LAP3), Department of Environmental Science and Engineering, Fudan University, Shanghai 200438, China

[2] Center for Environmental Measurement and Modeling, Office of Research and Development, U.S. Environmental Protection Agency, Research Triangle Park, North Carolina, USA

[3] Office of Air Quality Planning and Standards, Environmental Protection Agency, Research Triangle Park, NC 27711, United States

[4] Department of Atmospheric Chemistry and Climate, Institute of Physical Chemistry Rocasolano, CSIC, Madrid 28006, Spain

TOC ART

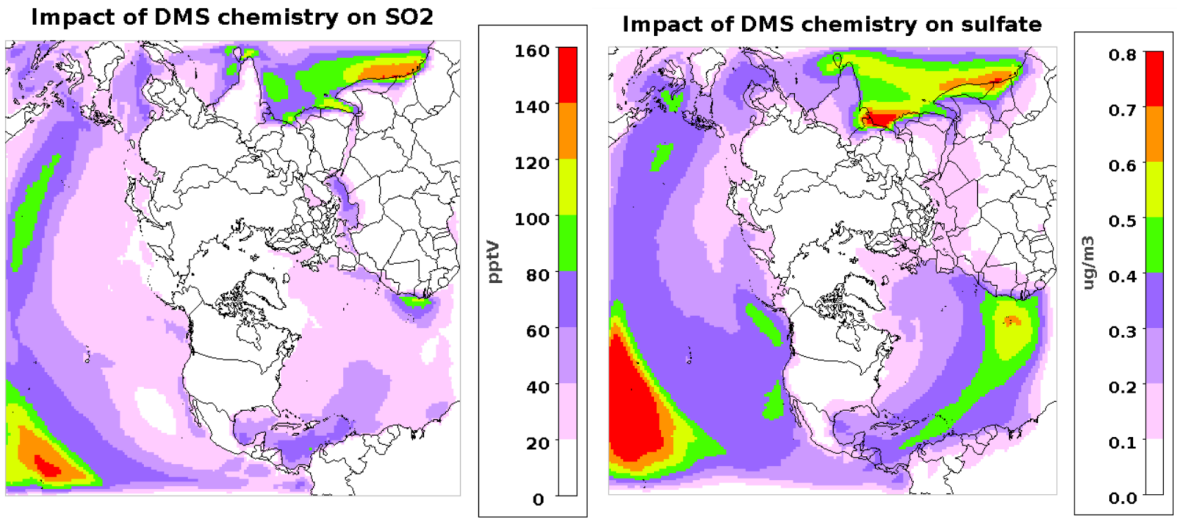
Impact of DMS chemistry on SO2
160
140
120
100
80
60
40
20
0
pptV
Impact of DMS chemistry on sulfate
0.8
0.7
0.6
0.5
0.4
0.3
0.2
0.1
0.0
ug/m3

ABSTRACT

We implement oceanic dimethylsulfide (DMS) emissions and its atmospheric chemical reactions into the Community Multiscale Air Quality (CMAQv53) model and perform annual simulations without and with DMS chemistry over the Northern Hemisphere. The model without the DMS chemistry predicts low concentrations of sulfur dioxide (SO_2) and sulfate (SO_4^{2-}) over seawater. DMS chemistry enhances both SO_2 and SO_4^{2-} over seawater and coastal areas. The largest enhancements occur at the surface with an annual mean surface SO_2 concentration enhancement of ~90% and SO_4^{2-} of ~30% over seawater compared to simulations without the DMS chemistry. The enhancements decrease with altitude and are limited to the lower atmosphere. The impact of DMS chemistry on SO_4^{2-} is largest in the summer and lowest in the fall due to the seasonality of DMS emissions and atmospheric photochemistry. Oceanic DMS enhances annual average SO_2 by 6 pptv and SO_4^{2-} by 0.09 μg/m^3 over the entire U.S. The hydroxyl and nitrate radical-initiated pathways oxidize 75% of the DMS while the halogens-initiated pathways oxidize 25%. DMS chemistry decreases aerosol pH and atmospheric visibility over seawater and coastal areas due to the enhancement of SO_4^{2-}. DMS chemistry generally captures the observed methanesulfonic acid to nss-SO_4^{2-} ratio.

Keywords: Dimethylsulfide, seawater, emissions, sulfur dioxide, sulfate

1.0 INTRODUCTION

In the 30+ years since Charlson et al. (1987) hypothesized that biogenically-produced dimethyl sulfide (DMS) from marine phytoplankton participates in a negative climate feedback loop affecting cloud condensation nuclei and cloudiness, the study of DMS from the world's oceans has been a vigorous area of research. Though the CLAW hypothesis (named after the authors of Charlson et al., 1987) has been criticized as too simplistic (Quinn and Bates, 2011), the resulting knowledge gained about the sources, oceanic concentrations, and emissions of oceanic DMS has enabled chemical transport and earth systems models to realistically simulate its impacts on air quality and climate. DMS in the ocean is produced from the breakdown of dimethylsulfoniopropionate (DMSP) generated from microalgal metabolic processes and exudation/mortality (Stefels et al., 2007). The concentration of DMS in seawater has been sampled extensively, leading to the construction of the Global Surface Seawater DMS Database (http://saga.pmel.noaa.gov/dms) and interpolated estimates of the global concentration distribution (Kettle et al., 1999; Kettle and Andreae, 2000). An updated climatology of oceanic DMS concentrations using over 47,000 measurements was reported by Lana et al. (2011).

Chemical transport and earth systems models typically utilize oceanic DMS climatology along with parameterizations of the sea-to-air transfer velocity based on surface wind speed to simulate DMS emissions from the ocean (Rasch et al., 2000; Chin et al., 2000; Park et al., 2004). Regional air quality models such as Community Multiscale Air Quality (CMAQ, https://www.epa.gov/cmaq) have historically not included oceanic DMS emissions because of their 1) typical application to high pollution areas violating air quality standards, 2) relatively high anthropogenic emissions of sulfur dioxide (SO_2) resulting in sulfate (SO_4^{2-}) concentrations that overwhelm the DMS contribution, and 3) small fraction of oceanic area in a typical model domain. Smith and Mueller (2010) implemented several natural sulfur emission sources including oceanic DMS into the CMAQ model for a domain covering the continental U.S., southern Canada, and northern Mexico and surrounding oceans based on the year 2002. For that domain and simulation year, natural gaseous sulfur emissions made up only 16% of the total gaseous sulfur emissions but increased SO_4^{2-} concentrations over oceanic and inland regions by as much as 2 and 0.1-0.2 μg m^{-3}, respectively (Mueller et al., 2011). Mueller and Mallard (2011) found that natural SO_4^{2-} concentrations predicted by CMAQ with DMS and other natural sulfur sources were slightly overpredicted in the western U.S. and well predicted in the eastern U.S. when compared with natural condition values used in the Regional Haze Rule. Mueller and Mallard (2011) also reported that natural SO_4^{2-} as a percentage of total SO_4^{2-} was >60% over much of the Pacific Ocean within the domain and between 20% and 60% over the western U.S.

In recent years, changes to both air quality and the Regional Haze Rule have led to a renewed interest by the United States Environmental Protection Agency (EPA) in quantifying the contribution of DMS to natural SO_4^{2-} concentrations. In terms of air quality, the substantial reduction in SO_2 emissions from power plants in the U.S. (https://www3.epa.gov/airmarkets/progress/datatren ds/index.html) and resulting decrease in SO_4^{2-} concentrations (Chan et al., 2018) has led to increases in the fraction of sulfur from natural sources across the U.S. Furthermore, differentiating natural and anthropogenic sources of haze is an important component of the recommended metric for tracking visibility progress in the Regional Haze Rule (Gantt et al., 2018; EPA, 2018). In the recommended metric, the 20% most impaired days used to track visibility have the highest anthropogenic extinction relative to natural extinction. Because air quality models used to support the Regional Haze Rule need to accurately differentiate the natural and anthropogenic sources of haze, previously overlooked natural sources such as DMS have gained renewed attention. In this work, oceanic DMS emissions and its atmospheric chemistry are implemented in the CMAQ model and simulated for the year 2016.

2.0 METHODOLOGY

2.1 Model description

The CMAQ model (https://www.epa.gov/cmaq) is a widely used air quality modeling system (Kang et al., 2013; Sarwar et al., 2014; Foley et al., 2015; Appel et al., 2017; Gantt et al., 2017) containing interactions of multiple complex emission inventories and atmospheric processes. Applications of the CMAQ model have ranged from state-of-the-science air quality research to regulatory efforts such as reviews of the Ozone and Particulate Matter National Ambient Air Quality Standards. To assess the impact of DMS chemistry on air quality across the Northern Hemisphere, we performed simulations for the year 2016 using the offline hemispheric version (Mathur et al., 2017) of CMAQ v5.3 with a three-month spin-up period in 2015. The simulation uses a horizontal grid resolution of 108 km and 44 vertical layers up to 50 hPa. The CMAQ model was configured to use aero7 as the aerosol module (includes semivolatile primary organic aerosols (POA) and empirical anthropogenic secondary organic aerosols (SOA) (Murphy et al. 2017), updated monoterpene SOA (Xu et al., 2018), and SOA from other systems including isoprene, benzene, toluene, xylene, alkanes, PAHs, and glyoxal + methylglyoxal (Pye et al., 2017)) and cb6r3 (Emery et al., 2015 and Luecken et al., 2019) as the gas-phase mechanism along with detailed halogen chemistry (Sarwar et al., 2019). The meteorological field for the model was generated using the Weather Research and Forecasting

(WRFv3.8) model (Skamarock and Klemp, 2008) and processed using the Meteorology-Chemistry Interface Processor (MCIP; Otte and Pleim, 2009). We use model-ready emissions for hemispheric CMAQ developed by Vukovich et al. (2018).

2.2 DMS emissions

The sea-air flux of DMS is estimated using gas transfer velocity and DMS concentrations in seawater as described in the Supplementary Information (Lana et al., 2011). Using the monthly mean climatological DMS concentrations in seawater of Lana et al. (2011) and the Liss and Merlivat (1986) parameterization, we estimate annual DMS emissions of 10.6 Tg(S) over the Northern Hemisphere. Our estimate compares favorably with the estimate of 10.8 Tg(S) reported by Lana et al. (2011) and with the estimates of 7.4-11.4 Tg(S) reported by Boucher et al. (2003). Annual estimates of global DMS emissions range between 15-34 Tg(s) (Kloster et al., 2006; Thomas et al., 2010; Hezel et al., 2011; Lana et al., 2011; Chen et al., 2018). DMS emission estimates for the Northern Hemisphere are generally lower than the estimates for the Southern Hemisphere because plankton species in the Southern Hemisphere produce more DMSP which is the main source of DMS (Kloster et al., 2006). Annual anthropogenic SO_2 emissions in the model are ~40 Tg(S). Thus, DMS contributed 26% of the total anthropogenic sulfur emissions in our model. The contribution of DMS emissions to the total global sulfur emissions is increasing as anthropogenic SO_2 emissions are decreasing due to world-wide regulatory actions. The highest DMS emissions in the Northern Hemisphere occur in the winter and summer and the lowest in the spring and fall (Figure S.1a). This is due to the higher wind speed driving the emissions in winter and higher seawater DMS concentrations driving the emissions in the summer. Relatively lower wind speed (compared to winter) and seawater DMS concentrations (compared to summer) in the spring and fall lead to reduced DMS emissions in those seasons.

2.3 DMS chemistry

Seven gas-phase chemical reactions related to DMS are incorporated in CMAQv5.3 (Table S.1). These reactions involve oxidation of DMS by hydroxyl radical (OH), nitrate radical (NO_3), chlorine radical (Cl), chlorine monoxide (ClO), iodine monoxide (IO), and bromine monoxide (BrO) to produce SO_2 and methanesulfonic acid (MSA). The primary sink of DMS occurs by reactions with OH during daytime (via two channels: H-abstraction and addition pathways) and NO_3 radicals at nighttime (Wilson and Hirst, 1996). NO_3 is more abundant in polluted areas due to oxides of nitrogen (NO_x) emissions from anthropogenic activities, while in clean marine conditions OH is the dominant oxidant of DMS. The H-abstraction primarily leads to SO_2, while the addition of OH forms SO_2 and MSA. We add R1-R3 following Chin et

al. (1996) with updated reaction rate constants from Sander et al. (2011). Hoffmann et al., (2016) reported that DMS oxidation by halogens oxides are ignored in current model parameterizations of atmospheric chemistry. DMS oxidation by halogens oxides are known to occur in the atmosphere and treated as a potential sink of DMS (Barnes et al., 1989; Sayin and McKee, 2004). We added R4-R7 using rate constants suggested by Atkinson (2006) and simulate BrO, ClO, IO and Cl concentrations using the detailed halogen chemistry recently incorporated into CMAQ (Sarwar et al., 2012; Sarwar et al., 2014; Sarwar et al., 2015; Sarwar et al., 2019). Another sink of DMS is the reaction between Cl and DMS, which could play an important role in coastal areas where Cl mixing ratios can reach high levels due to surf zone sea spray emissions and dechlorination of sea spray by anthropogenic pollutants. CMAQ contains one gas-phase reaction involving OH and five aqueous-phase chemical reactions involving hydrogen peroxide (H_2O_2), ozone (O_3), metal catalysis (iron/manganese), methylhydroperoxide (MHP), and peroxyacetic acid (PACD) for oxidation of SO_2 into SO_4^{2-} (Sarwar et al., 2011). Once SO_2 is produced by the oxidation of DMS, subsequent reactions in CMAQ then transform SO_2 into SO_4^{2-}. In our model, MSA produced from DMS can undergo dry and wet deposition but cannot form aerosols. Veres et al. (2020) recently analyzed data from airborne observations and reported a new DMS oxidation product (identified as hydroperoxy methyl thioformate). They developed a new DMS oxidation scheme by including the formation of hydroperoxy methyl thioformate, implemented it into a global model (CAM-Chem), and reported that the new scheme slows the formation SO_2 as well as SO_4^{2-} at surface between 60°N and 60°S and increases in other parts of the Earth compared to the traditional DMS oxidation scheme. This new scheme is not included in our study.

2.4 Simulation details

We performed two different annual simulations to investigate the importance of the DMS chemistry and its impact on air quality. One simulation used the CB6r3 chemical mechanism along with the halogen chemistry but without any DMS chemistry while the other simulation used the CB6r3 along with the halogen and the DMS chemistry. Differences in model results between the simulations can be attributed solely to the DMS chemistry. We employed the Integrated Reaction Rate (IRR) option in the model which enables estimates of the relative contribution of each reaction to the total DMS oxidation rate.

3.0 RESULTS AND DISCUSSSION

3.1 Impacts on annual mean SO_2 and SO_4^{2-} over seawater

Annual mean DMS concentrations over seawater with DMS chemistry are shown in Figure 1(a). DMS concentrations peak around 110 ppt at the surface and rapidly decrease with altitude reaching values < 5ppt at an altitude of 2 km. This result is consistent with Khan et al. (2016) and Chen et al. (2018) who reported that DMS mainly exists in the lower atmosphere (2-5 km). The vertical distributions of annual mean SO_2 and SO_4^{2-} concentrations without and with DMS chemistry over seawater are presented in Figure 1(a) and 1(b), respectively. The enhancements of SO_2 and SO_4^{2-} concentrations by the DMS chemistry are the highest at the surface and decrease with altitude. The impacts on SO_2 and $SO_4^{2-}$are limited to the lower troposphere. DMS chemistry increases surface SO_2 concentration by ~90% and surface SO_4^{2-}concentration by ~30% over seawater.

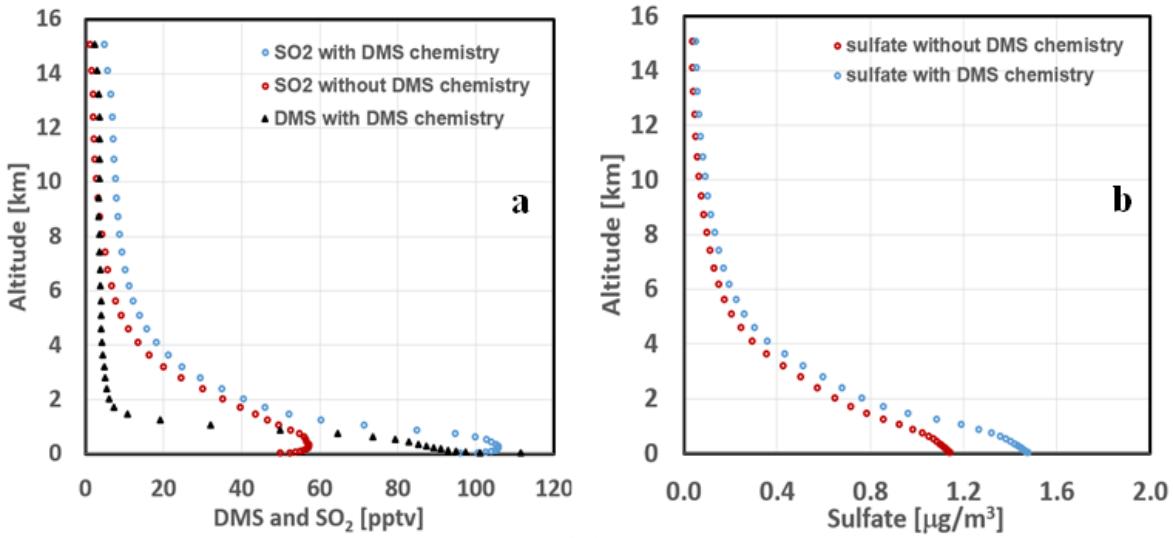

Figure 1: (a) Annual mean DMS concentration with DMS chemistry and SO_2 concentrations over seawater without and with DMS chemistry with altitude and (b) annual mean SO_4^{2-}concentrations over seawater without and with DMS chemistry with altitude

Analysis of the IRR results suggests that 63.5% of DMS is oxidized by OH (33.0% via abstraction channel and 30.5% via addition channel) which are within the ranges (52%-85%) reported by previous studies (Berglen et al., 2004; Boucher et al., 2003; Chen et al., 2018; Khan et al., 2016; Kloster et al., 2006). The oxidation of DMS by NO_3 accounts for 11.8%. Previous studies reported that NO_3 can account for 15%-29% of DMS oxidation (Berglen et al., 2004; Boucher et al., 2003; Chen et al., 2018; Khan et al., 2016; Kloster et al., 2006). The contribution of NO_3 to the total DMS oxidation is slightly lower than those studies due to lower abundance of DMS over the Northern Hemisphere. BrO, Cl, IO and ClO oxidation pathways contributed 16.0%, 8.2%, 0.4% and 0.1% to the total DMS oxidation, respectively. The BrO oxidation of DMS is similar to the ranges (12-16%) reported by Breider et al. (2010) and Chen et al. (2018). Consistent with these findings, our results also suggest that OH and NO_3 are responsible for the majority (~75%) of the DMS oxidation but that halogen-initiated pathways are also

important processes accounting for ~25% of DMS oxidation. In our simulations NO_3 is the only night-time oxidant of DMS; therefore, the magnitude of daytime DMS oxidation is far greater than that of the nighttime.

3.2 Spatial distribution of the DMS impacts on SO_2 and SO_4^{2-}

The annual DMS emission flux and annual mean surface DMS concentrations are presented in Figure S.2a and Figure S.2b, respectively. The surface DMS concentration ranges up to ~400 pptv with a mean value of ~110 pptv over seawater. The higher predicted values of DMS concentrations occur over lower latitude oceanic areas compared to those over higher latitude oceanic areas, which generally agree with the predicted high DMS emissions in the same areas. Concentrations over the Indian Ocean can reach high levels (75-375 pptv) due to the large oceanic production of DMS along with strong sea surface winds. The emissions of DMS depend on the sea surface winds, sea surface temperature, and oceanic productivity (Keller et al., 1989; Lana et al., 2011). However, the spatial distribution of DMS concentration does not exactly follow the emission distribution pattern due to the variation in DMS oxidation in different regions. For example, higher DMS concentrations are predicted in the vicinity of Norwegian Sea despite lower emission flux in that area due to low OH abundance at high latitudes (Lelieveld et al., 2016). Predicted DMS concentrations are lower over land than over seawater. DMS concentrations ranging up to ~100 pptv are predicted over some coastal areas of Northern Hemisphere while concentrations up to ~30 pptv are modeled over coastal areas of North America.

Annual mean surface SO_2 and SO_4^{2-} concentrations without DMS chemistry over the Northern Hemisphere are presented in Figures 2(a) and 2(c), respectively. High SO_2 and SO_4^{2-}concentrations are predicted over land due to anthropogenic sources, most pronounced over industrial areas of Europe, North America, India and China. Relatively higher levels of SO_2 and $SO_4^{2-}$are predicted over seawater in areas of commercial shipping lanes. Very low SO_2 and SO_4^{2-}concentrations are predicted over remote oceanic areas without the DMS chemistry. Annual mean surface SO_2 and SO_4^{2-} enhancements by the DMS chemistry are presented in Figures 2(b) and 2(d), respectively. DMS chemistry increases atmospheric SO_2 concentrations by 20-140 pptv and SO_4^{2-} concentrations by 0.1-0.8 μg/m^3 over most areas of seawater. For SO_2, such enhancements are higher over low latitude areas and some coastal areas due to higher DMS concentrations and higher oxidant levels. The annual mean contribution of DMS to SO_2 concentration over seawater is ~46 pptv, which is lower than 130 pptv over Northern Hemisphere reported by Gondwe et al. (2003) due to differences between models, DMS emission flux estimates, and reaction rate constants in the two studies. The pattern of SO_4^{2-}

concentration enhancement by DMS is similar to that of the SO_2 enhancement. However, the high values are not limited to the areas with large DMS emission flux as it can transport to larger geographical range due to longer atmospheric residence time of particles. DMS chemistry also decreases aerosol nitrate concentrations by 0.1-0.3 μg/m^3 (not shown) over a large area of seawater due to the limited availability of ammonia. On average, such decreases (-0.07 μg/m^3) of nitrate over seawater are lower than the enhancement (+0.33 μg/m^3) of SO_4^{2-}.

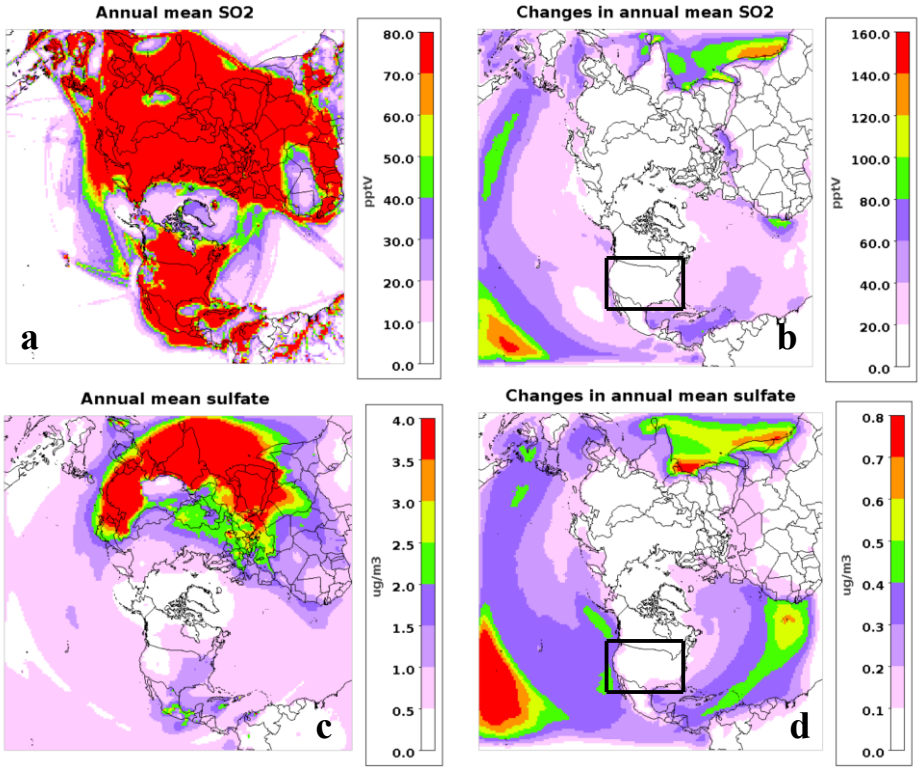

Figure 2: Spatial distribution of (a) annual mean surface SO_2, (b) annual mean surface SO_2 enhancement by the DMS chemistry, (c) annual mean surface SO_4^{2-}, (d) annual mean surface SO_4^{2-}enhancement by the DMS chemistry over Northern Hemisphere. The black box is the area over which enhancements are shown in Figure 4.

3.3 Seasonal variation of the SO_2 and SO_4^{2-}enhancements by DMS chemistry

Seasonal mean atmospheric DMS concentrations over seawater are shown in Figure 3(a). The highest DMS concentrations occur in winter, followed closely by the summertime concentrations. The spring and fall have substantially lower DMS concentrations over seawater. The seasonal variation of DMS concentrations generally follows the seasonality of DMS emissions. Seasonal SO_2 and SO_4^{2-} enhancements over seawater by DMS chemistry are shown in Figure 3(b) and 3(c), respectively. The largest SO_2 enhancement occurs in the winter and summer months while the minimum enhancement occurs in spring and fall, closely following that of DMS concentrations. The seasonality of SO_4^{2-} enhancement from DMS is distinct, with the largest enhancement occurring in summer followed by winter and spring and the lowest enhancement in the fall. Because the conversion of SO_2 into SO_4^{2-} occurs mainly via gas-phase reaction with OH and aqueous-phase reactions with H_2O_2 and O_3, the higher

summertime concentrations of OH and H_2O_2 facilitates the conversion of SO_2 into SO_4^{2-}. The combination of higher oxidant concentrations and relatively higher SO_2 enhancement produces the highest enhancement of SO_4^{2-} in summer.

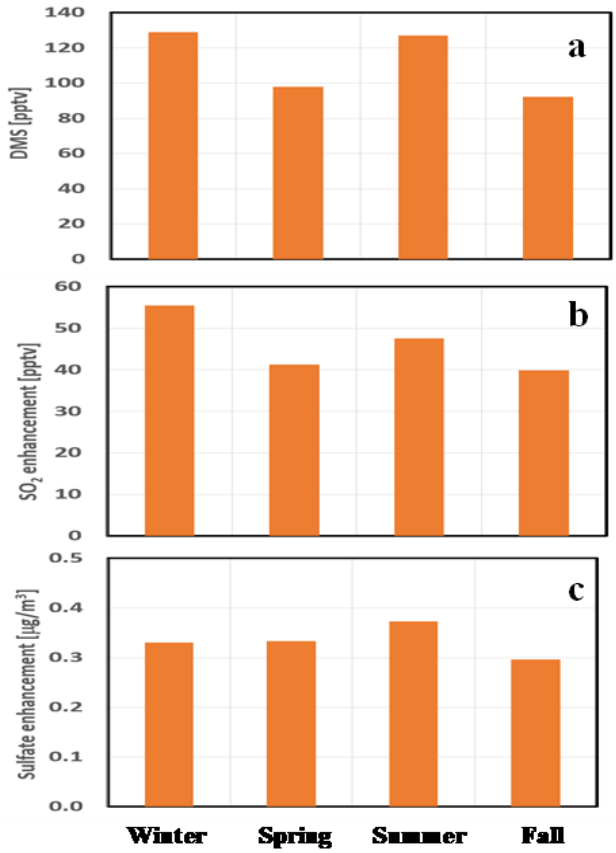

Figure 3: (a) Seasonal variation of DMS concentration, (b) seasonal variation of the SO_2 enhancement by DMS chemistry, and (c) seasonal variation of the SO_4^{2-} enhancement by DMS chemistry over seawater. Winter represents months of December-February, spring represents months of March-May, summer represents months of June-August, and fall represents months of September-November.

3.4 MSA/nss-SO_4^{2-} ratio

DMS is the only known precursor of MSA, while non-sea-salt SO_4^{2-} (nss-SO_4^{2-}) is produced from the oxidation of both anthropogenic and biogenically produced SO_2. Therefore, the MSA to nss-SO_4^{2-} ratio has been used in previous studies to assess the importance of biogenic SO_4^{2-}. Higher values of the ratio indicate larger contribution from biogenic sources while lower values reveal smaller contributions. The spatial distribution of the model-calculated MSA to nss-SO_4^{2-} ratio is presented in Figure S.3a. We use CMAQ predicted MSA and calculate nss-SO_4^{2-} as follows: nss-SO_4^{2-} = SO_4^{2-}- 0.2514 × Na^+; Na^+ is sodium concentration and 0.2514 represents SO_4^{2-} to Na^+ ratio in seawater. Higher values are predicted over the low latitude areas of the Pacific Ocean and areas of the Atlantic and Indian Oceans signifying the larger importance of biogenic sources. Lower values are predicted near many coastal and high latitude areas

suggesting the domination of anthropogenic sources in these areas. We compared model predictions with long-term observed data from Gonde et al. (2004) which Chen et al. (2018) also used in their study. The model generally captures the observed trend (Figure S.3b); however, some predicted values differ from the observed data by a factor of up to ~2 due primarily to the fact that we do not use multiphase DMS chemistry which has been shown to be important for reproducing these ratios (Chen et al., 2018).

3.5 Interactions of DMS chemistry on aerosol pH

Acidity is an important property of aerosols that can affect human health, deposition, and climate. We estimated fine-mode aerosol acidity (pH_F) without and with DMS chemistry following the procedures described in Pye et al. (2020). Predicted annual average pH_F levels (without DMS) range between 0.0-5.0 over land and are largely driven by variability in ammonia and nonvolatile cation emissions from sources such as dust (Figure S.4a). Dust outflow and sea-spray rich regions have pH_F values approaching 6.0 without the presence of DMS. Locations over seawater influenced by anthropogenic activity, such as urban outflow or ships, experience pH_F values approaching 1.0. Predicted levels are similar to the values reported by Pye et al. (2020) which contains a detailed discussion on the drivers of acidity.

DMS chemistry leads to more acidic particles over seawater (Figure S.4b) due to the enhancement of SO_2 which eventually leads to additional SO_4^{2-}, H^+, and lower aerosol pH_F. Aerosol pH_F is reduced by 0.5-1.5 over most seawater areas, except in locations with little influence from dust or anthropogenic emissions (low latitude areas of the Pacific Ocean) where the pH_F is reduced by 1.5-2.5. The exception to this reduction in pH_F is in areas of African dust outflow over the Atlantic Ocean where pH_F is mainly dictated by nonvolatile cations in dust. Acidity changes of pH_F values of 0.5 or less cannot be evaluated using current observations since differences in pH approximations of different models are of similar magnitude (Pye et al., 2020). pH_F changes > 0.5 could be evaluated, however, only three observations are available for marine environments in the Northern Hemisphere and all coincide with small changes in modeled pH_F due to DMS chemistry (Barbados pH_F = 2.8, Hawaii-volcanic influenced pH_F = 1.1, Hawaii-marine influenced pH_F = 4.6; Pye et al., 2020).

Aqueous-phase oxidation of dissolved SO_2 to SO_4^{2-} in CMAQ occurs entirely in clouds (no aqueous-phase particle reactions). The spatial pattern of SO_2 and SO_4^{2-} changes (Figure 2b and 2d) suggests that SO_2 produced from DMS may be more efficiently converted to SO_4^{2-} in locations where clouds are less acidic such as in Saharan outflow and over the northern low latitudes that have cloud water pH values above 6 (Pye et al., 2020). O_3 and transition metal

catalyzed SO_2 oxidation reactions occur rapidly at these pH values. As a result, SO_2 from DMS formed in these locations has a higher probability of being converted to SO_4^{2-}.

3.6 Impacts of DMS chemistry on atmospheric visibility

DMS contributes to visibility impairment as a natural source of SO_4^{2-}. To quantify the impact of DMS on visibility, we calculate extinction following Pitchford et al. (2007) which uses an empirical equation to estimate light extinction from species-specific coefficients and site-specific hygroscopic growth factors. The species-specific coefficients are used, with the exception of nitrogen dioxide extinction and Rayleigh scattering which are not included. We use WRF estimated relative humidity (RH) for growth factor calculations to produce continuous spatial maps of the mean ammonium sulfate extinction for August because DMS chemistry has the largest impact on SO_4^{2-} in summer (Figure 3c). Figure S.5a shows the percent changes in ammonium sulfate extinction due to the DMS chemistry. Large increases are evident over the oceans with factor of two increases over much of the Pacific Ocean. Although increases in ammonium sulfate extinction are smaller (less than 30%) over the mainland of the continents, coastal zones and peninsulas have relatively large ammonium sulfate extinction impacts from DMS chemistry. Figure S.5b shows that these increases in ammonium sulfate extinction are partially offset by decreased ammonium nitrate extinction. Figure S.5c shows a moderate net increase in the total extinction due to DMS chemistry that is largest near the Pacific Northwest coast.

The Interagency Monitoring of Protected Visual Environments (IMPROVE) (http://vista.cira.colostate.edu/Improve) operates numerous monitors in the U.S. which measure extinction. We calculate extinction for annual as well as the 20% most impaired days used in the Regional Haze visibility tracking metric (EPA, 2018) and compared them to the observed data from monitors located near the Alaska coast, the Pacific Ocean coast, and the Gulf of Mexico coast. For calculating extinction for these monitors, we use climatological growth factors from the IMPROVE website and calculate the Normalized Mean Bias (NMB) using equation 1 (Eder and Yu, 2006) (Y_d is the model calculated value and O_d is observed value, N is the daily sample size). NMB for the model without (NMB_{BASE}) and with DMS chemistry (NMB_{DMS}) are used to show the impacts on model performance.

$$NMB = 100 \times \frac{\sum_{d=1}^{N}(Y_d - O_d)}{\sum_{d=1}^{N} O_d} \quad (1)$$

At the Alaska and Pacific coast sites, the model simulation without DMS chemistry overpredicts annual extinction from both ammonium sulfate and ammonium nitrate (Table S.2). Adding DMS, degrades the annual performance for ammonium sulfate but moderately

improves for ammonium nitrate at both coastal sites. For the 20% most impaired days, adding DMS tends to improve the model performance for both ammonium sulfate and ammonium nitrate extinction at the Alaska coast sites and deteriorates the performance for both ammonium sulfate and ammonium nitrate extinction at the pacific coast. At the Gulf of Mexico sites, adding DMS moderately improves performance of annual extinction for ammonium sulfate but degrades the ammonium nitrate extinction with similar results on the 20% most impaired days. The impact of DMS chemistry on total extinction at the coastal sites is small due to the offsetting ammonium sulfate and ammonium nitrogen extinction change, and slightly degrades the existing overprediction without DMS model simulation.

3.7 Impacts of DMS chemistry on SO_2 and SO_4^{2-} enhancements over the U.S.

Annual mean SO_2 and SO_4^{2-} enhancements by DMS chemistry over the U.S. are presented in Figures 4(a) and 4(b), respectively. Relatively moderate impacts on annual average SO_2 and SO_4^{2-} concentrations are predicted, with the largest enhancements of 10-30 pptv for SO_2 and 0.1-0.3 μg/m^3 for SO_4^{2-} occurring along the U.S. coastlines. Enhancements are less than 10 pptv for SO_2 and 0.1 μg/m^3 for SO_4^{2-} in the interior portions of the U.S. On average, DMS chemistry enhances annual mean SO_2 by 6 pptv and SO_4^{2-} by 0.09 μg/m^3 across the U.S. It enhances annual mean SO_2 by 10 pptv averaged over the Pacific coast states, 11 pptv over the Gulf coast states, and 8 pptv over the Atlantic coastal states. It enhances annual mean SO_4^{2-} by 0.15 μg/m^3 averaged over the Pacific coast states, 0.13 μg/m^3 over the Gulf coast states, and 0.09 μg/m^3 over the Atlantic coastal states. Our results are in qualitative agreement with the findings reported by Mueller et al. (2011) and Park et al. (2004) who reported that natural emissions enhance SO_4^{2-} by 0.1-0.2 μg/m^3 over south Texas and Florida, and 0.03-0.11 μg/m^3 over western and eastern U.S., respectively.

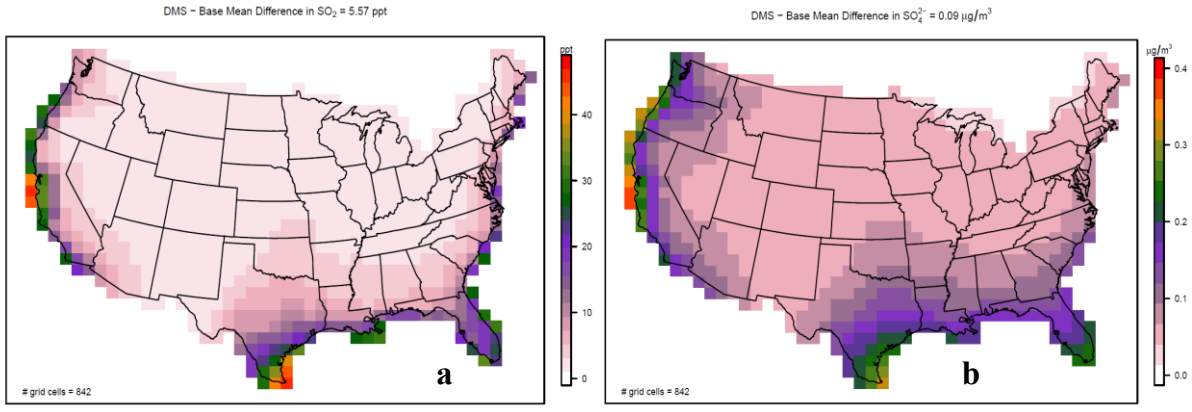

Figure 4: Spatial distribution of (a) annual mean surface SO_2 enhancement by the DMS chemistry over the U.S. and (b) annual mean surface SO_4^{2-} enhancement by the DMS chemistry over the U.S.

Predicted SO_4^{2-} concentrations are compared to observed data from the Clean Air Status and Trends Network (CASTNET), Chemical Speciation Network (CSN), and Interagency Monitoring of Protected Visual Environments (IMPROVE) sites (Figure S.6.1) to examine the impacts on model performance. For all sites in the U.S., predicted SO_4^{2-} concentrations without DMS chemistry are higher than observed values for most months except in July-September (Figure S.6.2). DMS chemistry degrades model performance for most months. However, these changes are relatively small due to the limited impact of DMS chemistry in the interior of the U.S. For the subset of coastal sites, however, DMS chemistry has a larger and more nuanced impact on model performance. DMS chemistry has mixed impact on the model performance at sites along the Alaska coast (Figure 5a), deteriorates the model performance by larger margins for most months at sites along the Pacific coast (Figure 5b), but improves the comparison with observed data for most months at the Gulf of Mexico sites (Figure 5c).

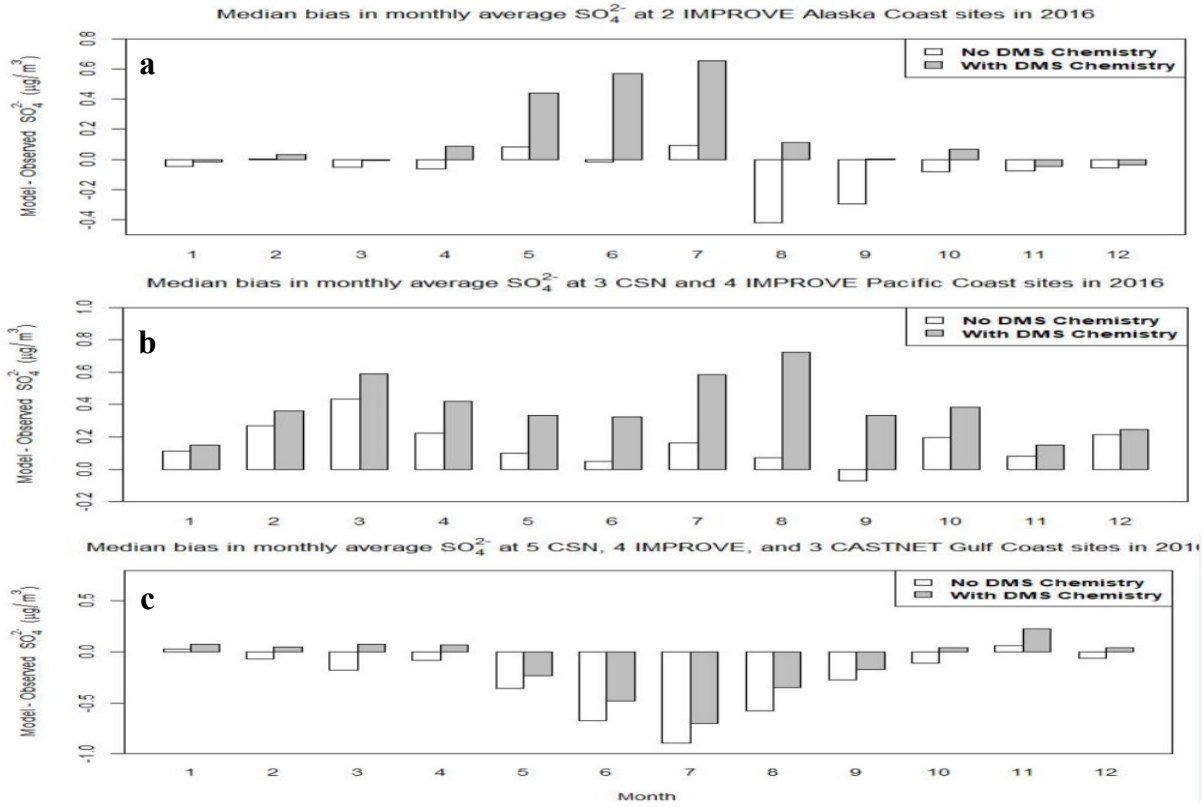

Figure 5: A comparison of median bias for monthly average SO_4^{2-} in the U.S: (a) Alaska coastal sites, (b) Pacific coast sites, and (c) Gulf of Mexico coast sites. All observations within a grid cell for a given month are used to calculate an observed monthly average for each grid cell containing at least one monitor. Then median bias between these observed monthly averages and the modeled monthly averages at those grid cells is calculated.

3.8 Future work

In this study, we have implemented oceanic emissions and gas-phase atmospheric chemistry of DMS in CMAQ over the Northern Hemisphere domain using a relatively large horizontal grid resolution. Future modeling studies using finer horizontal grid resolution may be needed

to further improve the impact of DMS chemistry over the U.S. Several recent studies have also advanced the understanding of DMS chemistry since we undertook this study. For example, Chen et al. (2017) reported that hydrobromic acid can oxidize dissolved SO_2 and potentially be an important source of SO_4^{2-} over seawater. Chen et al. (2018) suggested that multiphase chemistry of DMS is important for producing MSA. Veres et al. (2020) suggested a new DMS oxidation scheme that can produce hydroperoxy methyl thioformate. Future modeling studies using CMAQ to simulate DMS chemistry may need to incorporate these chemical reactions to properly predict the impact of DMS on MSA and sulfate concentrations in the model.

DISCLAIMER

The views expressed in this paper are those of the authors and do not necessarily represent the views or policies of the U.S. EPA. This manuscript has gone through review process within the Agency and cleared for publication.

References

Appel, K. W.; Napelenok, S. L.; Foley, K. M.; Pye, H. O. T.; Hogrefe, C.; Luecken, D. J.; Bash, J. O.; Roselle, S. J.; Pleim, J. E.; Foroutan, H.; Hutzell, W. T.; Pouliot, G. A.; Sarwar, G.; Fahey, K. M.; Gantt, B.; Gilliam, R. C.; Heath, N. K.; Kang, D.; Mathur, R.; Schwede, D. B.; Spero, T. L.; Wong, D. C.; Young, J. O., Description and evaluation of the Community Multiscale Air Quality (CMAQ) modeling system version 5.1. *Geosci. Model Dev.* **2017,** *10*, (4), 1703-1732.

Barnes, I.; Becker, K. H.; Martin, D.; Carlier, P.; Mouvier, G.; Jourdain, J. L.; Laverdet, G.; Le Bras, G., Impact of Halogen Oxides on Dimethyl Sulfide Oxidation in the Marine Atmosphere. In *Biogenic Sulfur in the Environment*, American Chemical Society: 1989; Vol. 393, pp 464-475.

Berglen, T. F.; Berntsen, T. K.; Isaksen, I. S. A.; Sundet, J. K., A global model of the coupled sulfur/oxidant chemistry in the troposphere: The sulfur cycle. *Journal of Geophysical Research: Atmospheres* **2004,** *109*, (D19).

Boucher, O.; Moulin, C.; Belviso, S.; Aumont, O.; Bopp, L.; Cosme, E.; von Kuhlmann, R.; Lawrence, M. G.; Pham, M.; Reddy, M. S.; Sciare, J.; Venkataraman, C., DMS atmospheric concentrations and sulphate aerosol indirect radiative forcing: a sensitivity study to the DMS source representation and oxidation. *Atmos. Chem. Phys.* **2003,** *3*, (1), 49-65.

Breider, T. J.; Chipperfield, M. P.; Richards, N. A. D.; Carslaw, K. S.; Mann, G. W.; Spracklen, D. V., Impact of BrO on dimethylsulfide in the remote marine boundary layer. *Geophysical Research Letters* **2010,** *37*, (2).

Charlson, R. J.; Lovelock, J. E.; Andreae, M. O.; Warren, S. G., Oceanic phytoplankton, atmospheric sulphur, cloud albedo and climate. *Nature* **1987,** *326*, (6114), 655-661.

Chan, E. A. W.; Gantt, B.; McDow, S. The reduction of summer sulfate and switch from summertime to wintertime $PM_{2.5}$ concentration maxima in the United States. Atmos. Environ. 2018, 175, 25−32.

Chen, Q.; Sherwen, T.; Evans, M.; Alexander, B., DMS oxidation and sulfur aerosol formation in the marine troposphere: a focus on reactive halogen and multiphase chemistry. *Atmos. Chem. Phys.* **2018,** *18*, (18), 13617-13637.

Chen, Q.; Schmidt, J. A.; Shah, V.; Jaeglé, L.; Sherwen, T.; Alexander, B., Sulfate production by reactive bromine: Implications for the global sulfur and reactive bromine budgets. *Geophysical Research Letters* **2017,** *44*, (13), 7069-7078.

Chin, M.; Jacob, D. J.; Gardner, G. M.; Foreman-Fowler, M. S.; Spiro, P. A.; Savoie, D. L., A global three-dimensional model of tropospheric sulfate. *Journal of Geophysical Research: Atmospheres* **1996,** *101*, (D13), 18667-18690.

Eder, B.; Yu, S., A performance evaluation of the 2004 release of Models-3 CMAQ. *Atmospheric Environment* **2006,** *40*, (26), 4811-4824.

Emery, C., Jung, J., Koo, B., & Yarwood, G. Improvements to CAMx Snow Cover Treatments and Carbon Bond Chemical Mechanism for Winter Ozone. Final Report prepared for Utah Department of Environmental Quality, Salt Lake City, UT 2015, prepared by Ramboll Environ, Novato, CA, August 2015.

EPA, 2018. Technical Guidance on Tracking Visibility Progress for the Second Implementation Period of the Regional Haze Program (No. EPA-454/R-18-010). U.S. Environmental Protection Agency, RTP, NC. URL: https://www.epa.gov/sites/production/files/2018-12/documents/technical_guidance_tracking_visibility_progress.pdf

Foley, K. M.; Hogrefe, C.; Pouliot, G.; Possiel, N.; Roselle, S. J.; Simon, H.; Timin, B., Dynamic evaluation of CMAQ part I: Separating the effects of changing emissions and changing meteorology on ozone levels between 2002 and 2005 in the eastern US. *Atmospheric Environment* **2015,** *103*, 247-255.

Gantt, B.; Sarwar, G.; Xing, J.; Simon, H.; Schwede, D.; Hutzell, W. T.; Mathur, R.; Saiz-Lopez, A., The Impact of Iodide-Mediated Ozone Deposition and Halogen Chemistry on Surface Ozone Concentrations Across the Continental United States. *Environmental Science & Technology* **2017,** *51*, (3), 1458-1466.

Gantt, B.; Beaver, M.; Timin, B.; Lorang, P., Recommended metric for tracking visibility progress in the Regional Haze Rule. *J Air Waste Manag Assoc* **2018,** *68*, (5), 438-445.

Gondwe, M.; Krol, M.; Gieskes, W.; Klaassen, W.; de Baar, H., The contribution of ocean-leaving DMS to the global atmospheric burdens of DMS, MSA, SO2, and NSS SO4=. *Global Biogeochemical Cycles* **2003,** *17*, (2).

Gondwe, M.; Krol, M.; Klaassen, W.; Gieskes, W.; de Baar, H., Comparison of modeled versus measured MSA:nss $SO4^{=}$ ratios: A global analysis. *Global Biogeochemical Cycles* **2004,** *18*, (2).

Hezel, P. J.; Alexander, B.; Bitz, C. M.; Steig, E. J.; Holmes, C. D.; Yang, X.; Sciare, J., Modeled methanesulfonic acid (MSA) deposition in Antarctica and its relationship to sea ice. *Journal of Geophysical Research: Atmospheres* **2011,** *116*, (D23).

Hoffmann, E. H.; Tilgner, A.; Schrödner, R.; Bräuer, P.; Wolke, R.; Herrmann, H., An advanced modeling study on the impacts and atmospheric implications of multiphase dimethyl sulfide chemistry. *Proceedings of the National Academy of Sciences* **2016,** *113*, (42), 11776.

Kang, D.; Hogrefe, C.; Foley, K. L.; Napelenok, S. L.; Mathur, R.; Trivikrama Rao, S., Application of the Kolmogorov–Zurbenko filter and the decoupled direct 3D method for the dynamic evaluation of a regional air quality model. *Atmospheric Environment* **2013,** *80*, 58-69.

Keller, M. D.; Bellows, W. K.; Guillard, R. R. L., Dimethyl Sulfide Production in Marine Phytoplankton. In *Biogenic Sulfur in the Environment*, American Chemical Society: 1989; Vol. 393, pp 167-182.

Kettle, A. J.; Andreae, M. O.; Amouroux, D.; Andreae, T. W.; Bates, T. S.; Berresheim, H.; Bingemer, H.; Boniforti, R.; Curran, M. A. J.; DiTullio, G. R.; Helas, G.; Jones, G. B.; Keller, M. D.; Kiene, R. P.; Leck, C.; Levasseur, M.; Malin, G.; Maspero, M.; Matrai, P.; McTaggart, A. R.; Mihalopoulos, N.; Nguyen, B. C.; Novo, A.; Putaud, J. P.; Rapsomanikis, S.; Roberts, G.; Schebeske, G.; Sharma, S.; Simó, R.; Staubes, R.; Turner, S.; Uher, G., A global database of sea surface dimethylsulfide (DMS) measurements and a procedure to predict sea surface DMS as a function of latitude, longitude, and month. *Global Biogeochemical Cycles* **1999,** *13*, (2), 399-444

Kettle, A. J.; Andreae, M. O., Flux of dimethylsulfide from the oceans: A comparison of updated data sets and flux models. *Journal of Geophysical Research: Atmospheres* **2000,** *105*, (D22), 26793-26808.

Khan, M. A. H.; Gillespie, S. M. P.; Razis, B.; Xiao, P.; Davies-Coleman, M. T.; Percival, C. J.; Derwent, R. G.; Dyke, J. M.; Ghosh, M. V.; Lee, E. P. F.; Shallcross, D. E., A modelling study of the atmospheric chemistry of DMS using the global model, STOCHEM-CRI. *Atmospheric Environment* **2016,** *127*, 69-79.

Kloster, S.; Feichter, J.; Maier-Reimer, E.; Six, K. D.; Stier, P.; Wetzel, P., DMS cycle in the marine ocean-atmosphere system – a global model study. *Biogeosciences* **2006,** *3*, (1), 29-51.

Lana, A.; Bell, T. G.; Simó, R.; Vallina, S. M.; Ballabrera-Poy, J.; Kettle, A. J.; Dachs, J.; Bopp, L.; Saltzman, E. S.; Stefels, J.; Johnson, J. E.; Liss, P. S., An updated climatology of surface dimethlysulfide concentrations and emission fluxes in the global ocean. *Global Biogeochemical Cycles* **2011,** *25*, (1).

Lelieveld, J.; Gromov, S.; Pozzer, A.; Taraborrelli, D., Global tropospheric hydroxyl distribution, budget and reactivity. *Atmos. Chem. Phys.* **2016,** *16*, (19), 12477-12493.

Luecken, D. J.; Yarwood, G.; Hutzell, W. T., Multipollutant modeling of ozone, reactive nitrogen and HAPs across the continental US with CMAQ-CB6. *Atmospheric Environment* **2019,** *201*, 62-72.

Mathur, R.; Xing, J.; Gilliam, R.; Sarwar, G.; Hogrefe, C.; Pleim, J.; Pouliot, G.; Roselle, S.; Spero, T. L.; Wong, D. C.; Young, J., Extending the Community Multiscale Air Quality (CMAQ) modeling system to hemispheric scales: overview of process considerations and initial applications. *Atmos. Chem. Phys.* **2017,** *17*, (20), 12449-12474.

McGillis, W. R.; Dacey, J. W. H.; Frew, N. M.; Bock, E. J.; Nelson, R. K., Water-air flux of dimethylsulfide. *Journal of Geophysical Research: Oceans* **2000,** *105*, (C1), 1187-1193.

Mueller, S. F.; Mallard, J. W., Contributions of Natural Emissions to Ozone and PM2.5 as Simulated by the Community Multiscale Air Quality (CMAQ) Model. *Environmental Science & Technology* **2011,** *45*, (11), 4817-4823

Mueller, S. F.; Mao, Q.; Mallard, J. W., Modeling natural emissions in the Community Multiscale Air Quality (CMAQ) model – Part 2: Modifications for simulating natural emissions. *Atmos. Chem. Phys.* **2011,** *11*, (1), 293-320.

Murphy, B. N.; Woody, M. C.; Jimenez, J. L.; Carlton, A. M. G.; Hayes, P. L.; Liu, S.; Ng, N. L.; Russell, L. M.; Setyan, A.; Xu, L.; Young, J.; Zaveri, R. A.; Zhang, Q.; Pye, H. O. T., Semivolatile POA and parameterized total combustion SOA in CMAQv5.2: impacts on source strength and partitioning. *Atmos. Chem. Phys.* **2017,** *17*, (18), 11107-11133.

Nightingale, P. D.; Malin, G.; Law, C. S.; Watson, A. J.; Liss, P. S.; Liddicoat, M. I.; Boutin, J.; Upstill-Goddard, R. C., In situ evaluation of air-sea gas exchange parameterizations using novel conservative and volatile tracers. *Global Biogeochemical Cycles* **2000,** *14*, (1), 373-387.

Otte, T. L.; Pleim, J. E., The Meteorology-Chemistry Interface Processor (MCIP) for the CMAQ modeling system: updates through MCIPv3.4.1. *Geosci. Model Dev.* **2010,** *3*, (1), 243-256.

Park, R. J.; Jacob, D. J.; Field, B. D.; Yantosca, R. M.; Chin, M., Natural and transboundary pollution influences on sulfate-nitrate-ammonium aerosols in the United States: Implications for policy. *Journal of Geophysical Research: Atmospheres* **2004,** *109*, (D15).

Pitchford, M.; Malm, W.; Schichtel, B.; Kumar, N.; Lowenthal, D.; Hand, J., Revised Algorithm for Estimating Light Extinction from IMPROVE Particle Speciation Data. *Journal of the Air & Waste Management Association* **2007,** *57*, (11), 1326-1336.

Pye, H. O. T.; Murphy, B. N.; Xu, L.; Ng, N. L.; Carlton, A. G.; Guo, H.; Weber, R.; Vasilakos, P.; Appel, K. W.; Budisulistiorini, S. H.; Surratt, J. D.; Nenes, A.; Hu, W.; Jimenez, J. L.; Isaacman-VanWertz, G.; Misztal, P. K.; Goldstein, A. H., On the implications of aerosol liquid water and phase separation for organic aerosol mass. *Atmos. Chem. Phys.* **2017,** *17*, (1), 343-369

Pye, H. O. T.; Nenes, A.; Alexander, B.; Ault, A. P.; Barth, M. C.; Clegg, S. L.; Collett Jr, J. L.; Fahey, K. M.; Hennigan, C. J.; Herrmann, H.; Kanakidou, M.; Kelly, J. T.; Ku, I. T.; McNeill, V. F.; Riemer, N.; Schaefer, T.; Shi, G.; Tilgner, A.; Walker, J. T.; Wang, T.; Weber, R.; Xing, J.; Zaveri, R. A.; Zuend, A., The acidity of atmospheric particles and clouds. *Atmos. Chem. Phys.* **2020,** *20*, (8), 4809-4888.

Quinn, P. K.; Bates, T. S., The case against climate regulation via oceanic phytoplankton sulphur emissions. *Nature* **2011,** *480*, (7375), 51-56.

Rasch, P. J.; Barth, M. C.; Kiehl, J. T.; Schwartz, S. E.; Benkovitz, C. M., A description of the global sulfur cycle and its controlling processes in the National Center for Atmospheric Research Community Climate Model, Version 3. *Journal of Geophysical Research: Atmospheres* **2000,** *105*, (D1), 1367-1385.

Sander, S.; Friedl, R.; Abbatt, J.; Barker, J.; Burkholder, J.; Golden, D.; Kolb, C.; Kurylo, M.; Moortgat, G.; Wine, P. J. J. p., Chemical kinetics and photochemical data for use in atmospheric studies, evaluation number 14. **2011,** *10*.

Sarwar, G.; Fahey, K.; Napelenok, S.; Roselle, S.; Mathur, R. In *Examining the impact of CMAQ model updates on aerosol sulfate predictions*, The 10th Annual CMAS Models-3 User's Conference, October, Chapel Hill, NC, 2011; 2011.

Sarwar, G.; Gantt, B.; Foley, K.; Fahey, K.; Spero, T. L.; Kang, D.; Mathur, R.; Foroutan, H.; Xing, J.; Sherwen, T.; Saiz-Lopez, A., Influence of bromine and iodine chemistry on annual, seasonal, diurnal, and background ozone: CMAQ simulations over the Northern Hemisphere. *Atmospheric Environment* **2019,** *213*, 395-404.

Sarwar, G.; Gantt, B.; Schwede, D.; Foley, K.; Mathur, R.; Saiz-Lopez, A., Impact of Enhanced Ozone Deposition and Halogen Chemistry on Tropospheric Ozone over the Northern Hemisphere. *Environmental Science & Technology* **2015,** *49*, (15), 9203-9211.

Sarwar, G.; Simon, H.; Bhave, P.; Yarwood, G., Examining the impact of heterogeneous nitryl chloride production on air quality across the United States. *Atmos. Chem. Phys.* **2012,** *12*, (14), 6455-6473.

Sarwar, G.; Simon, H.; Xing, J.; Mathur, R., Importance of tropospheric ClNO2 chemistry across the Northern Hemisphere. *Geophysical Research Letters* **2014,** *41*, (11), 4050-4058.

Sayin, H.; McKee, M. L., Computational Study of the Reactions between XO (X = Cl, Br, I) and Dimethyl Sulfide. *The Journal of Physical Chemistry A* **2004,** *108*, (37), 7613-7620.

Skamarock, W. C.; Klemp, J. B., A time-split nonhydrostatic atmospheric model for weather research and forecasting applications. *Journal of Computational Physics* **2008,** *227*, (7), 3465-3485

Smith, S. N.; Mueller, S. F., Modeling natural emissions in the Community Multiscale Air Quality (CMAQ) Model–I: building an emissions data base. *Atmos. Chem. Phys.* **2010,** *10*, (10), 4931-4952.

Stefels, J.; Steinke, M.; Turner, S.; Malin, G.; Belviso, S., Environmental constraints on the production and removal of the climatically active gas dimethylsulphide (DMS) and implications for ecosystem modelling. *Biogeochemistry* **2007,** *83*, (1), 245-275.

Thomas, M. A.; Suntharalingam, P.; Pozzoli, L.; Rast, S.; Devasthale, A.; Kloster, S.; Feichter, J.; Lenton, T. M., Quantification of DMS aerosol-cloud-climate interactions using the ECHAM5-HAMMOZ model in a current climate scenario. *Atmos. Chem. Phys.* **2010,** *10*, (15), 7425-7438.

Veres, P. R.; Neuman, J. A.; Bertram, T. H.; Assaf, E.; Wolfe, G. M.; Williamson, C. J.; Weinzierl, B.; Tilmes, S.; Thompson, C. R.; Thames, A. B.; Schroder, J. C.; Saiz-Lopez, A.; Rollins, A. W.; Roberts, J. M.; Price, D.; Peischl, J.; Nault, B. A.; Møller, K. H.; Miller, D. O.; Meinardi, S.; Li, Q.; Lamarque, J.-F.; Kupc, A.; Kjaergaard, H. G.; Kinnison, D.; Jimenez, J. L.; Jernigan, C. M.; Hornbrook, R. S.; Hills, A.; Dollner, M.; Day, D. A.; Cuevas, C. A.; Campuzano-Jost, P.; Burkholder, J.; Bui, T. P.; Brune, W. H.; Brown, S. S.; Brock, C. A.; Bourgeois, I.; Blake, D. R.; Apel, E. C.; Ryerson, T. B., Global airborne sampling reveals a previously unobserved dimethyl sulfide oxidation mechanism in the marine atmosphere. *Proceedings of the National Academy of Sciences* **2020,** *117*, (9), 4505.

Vukovich, J. M., Eyth, A., Henderson, B., Allen, C. and Beidler, J., 2018. Development of 2016 hemispheric emissions for CMAQ", the 17th Annual CMAS Models-3 User's Conference**, October,** Chapel Hill, NC, October 22-24, 2018 **(**https://www.cmascenter.org/conference/201 8/agenda.cfm; last accessed on 4/16/2020**)**

Wilson, C.; Hirst, D. M., Kinetics of gas phase oxidation of reduced sulfur compounds. *Progress in Reaction Kinetics* **1996,** *21*, (2-3), 69-132.

Xu, L.; Pye, H. O. T.; He, J.; Chen, Y.; Murphy, B. N.; Ng, N. L., Experimental and model estimates of the contributions from biogenic monoterpenes and sesquiterpenes to secondary organic aerosol in the southeastern United States. *Atmos. Chem. Phys.* **2018,** *18*, (17), 12613-12637.